

Supporting Information

Oxygen-Deficient Bimetallic oxide $M_{0.11}W_{0.89}O_{3-x}$ for Flexible Energy Storage and Electrochromic Applications

Pritha Dutta^{a,b,†}, Kavya V Palliyal^{a,d,†}, Ramya Prabhu^c, and Ashutosh K. Singh^{a,b,d,*}

^aCentre for Nano and Soft Matter Sciences, Bengaluru 562162, India.

^bManipal Academy of Higher Education, Manipal 576104, Karnataka, India.

^cPrayoga Institute of Education Research, Bengaluru, Karnataka 562112, India.

^dAcademy of Scientific and Innovative Research (AcSIR), Ghaziabad, Uttar Pradesh 201002, India.

†Contributed equally

*Corresponding author

E-mail address: Dr. Ashutosh K. Singh (aksingh@cens.res.in, ashuvishen@gmail.com)

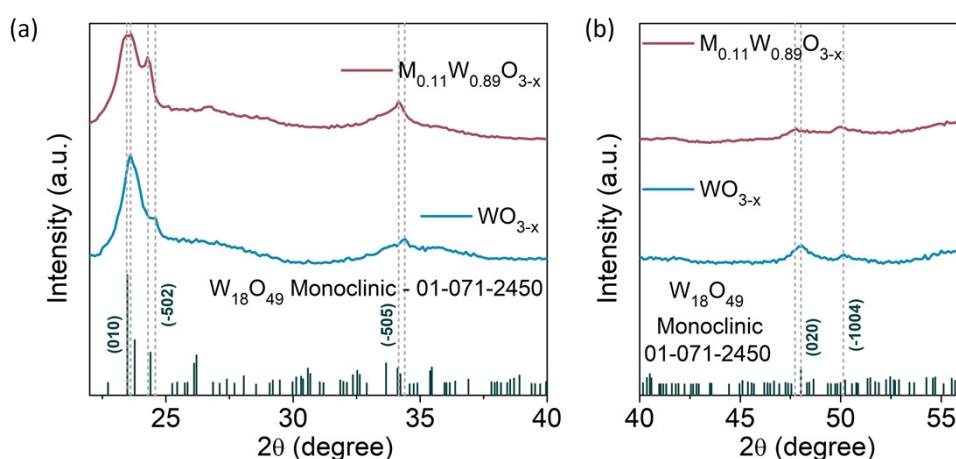


Figure S1. The comparison of XRD patterns between WO_{3-x} and $M_{0.11}W_{0.89}O_{3-x}$ with the reference JCPDS pattern in the 2θ range of (a) 22° to 40° and (b) 40° to 56° .

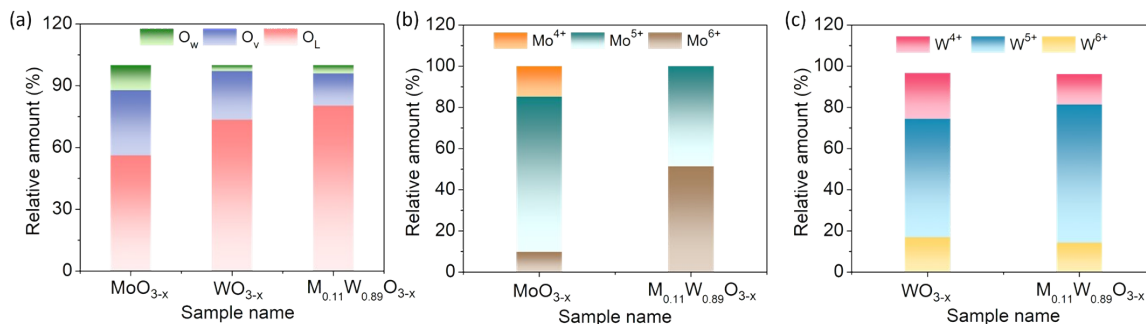


Figure S2. The bar diagram to compare the relative amounts from high-resolution XPS spectra – (a) O1s, (b) Mo3d, and (c) W4f.

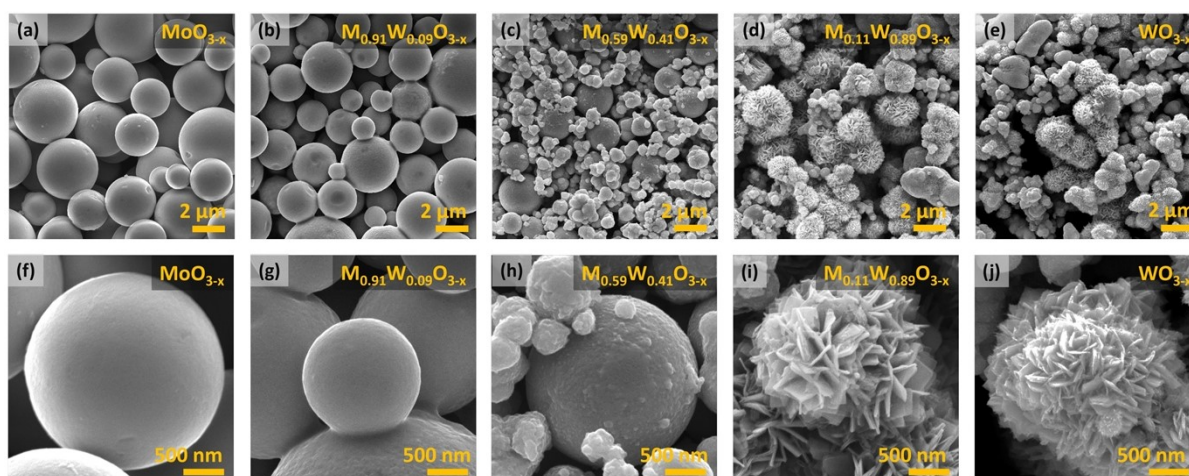


Figure S3. FESEM image of MoO_{3-x} at (a) low magnification and (f) high magnification; of M_{0.91}W_{0.09}O_{3-x} at (b) low magnification and (g) high magnification; of M_{0.59}W_{0.41}O_{3-x} at (c) low magnification and (h) high magnification; of M_{0.11}W_{0.89}O_{3-x} at (d) low magnification and (i) high magnification; and of WO_{3-x} at (e) low magnification and (j) high magnification.

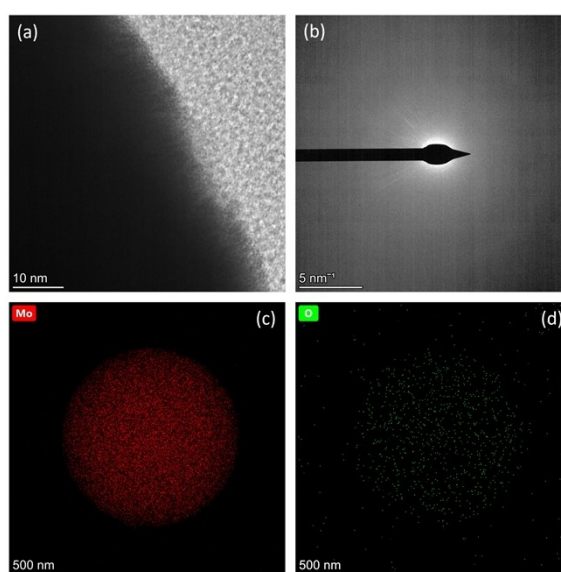


Figure S4. (a) HRTEM image, (b) SAED pattern, elemental mapping of (c) Mo and (d) O of the MoO_{3-x} sample.

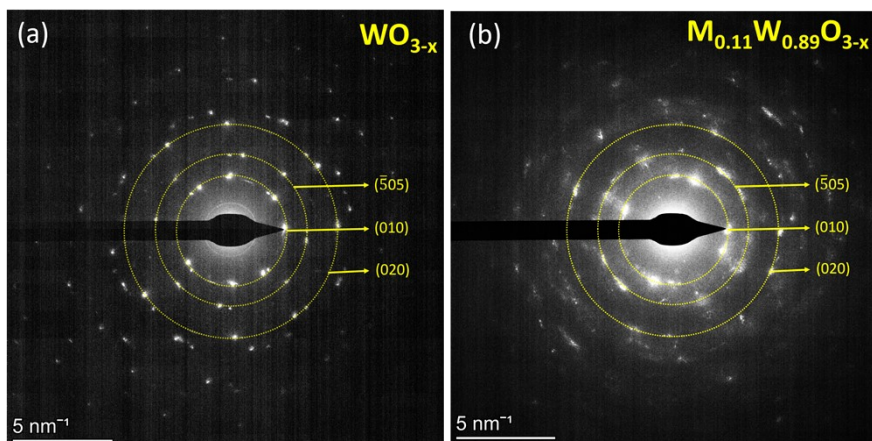


Figure S5. SAED patterns of (a) WO_{3-x} and (b) $\text{M}_{0.11}\text{W}_{0.89}\text{O}_{3-x}$.

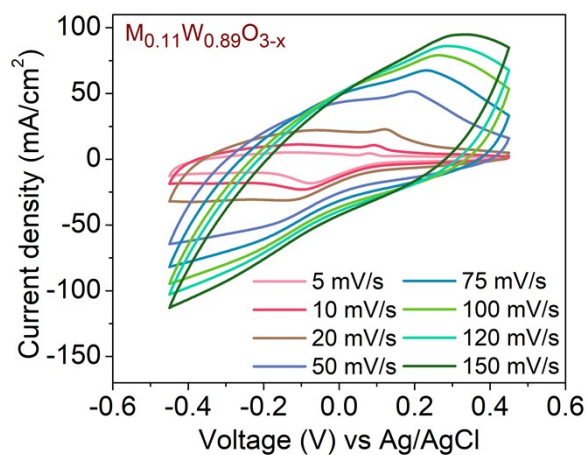


Figure S6. The CV profiles at different scan rates for the sample $\text{M}_{0.11}\text{W}_{0.89}\text{O}_{3-x}$.

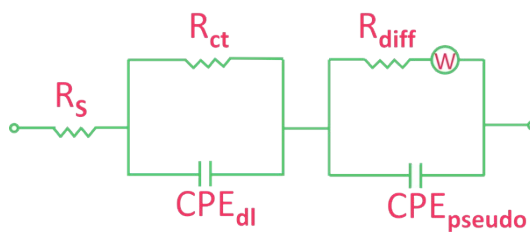


Figure S7. Equivalent circuit diagram for Nyquist plot.

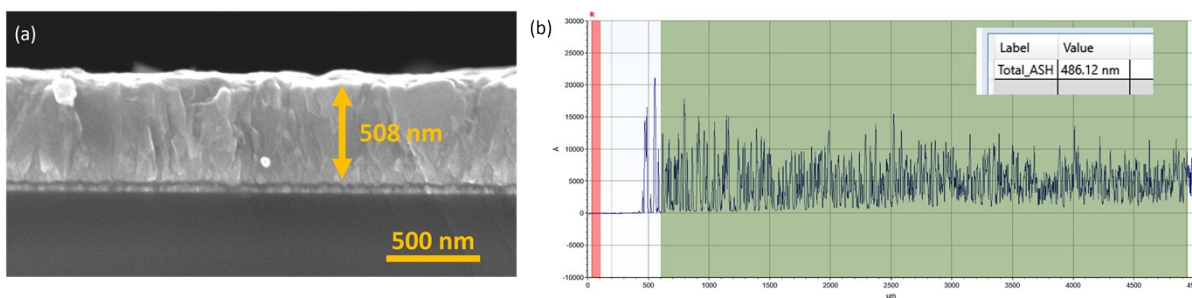


Figure S8. (a) Cross-sectional FESEM image and (b) thickness profile of the spray-coated $M_{0.11}W_{0.89}O_{3-x}$ electrode.

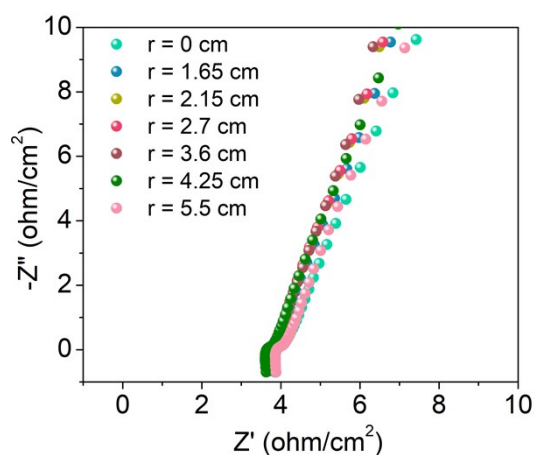


Figure S9. Nyquist plots of the flexible supercapacitor device, bent at different radii of curvature.

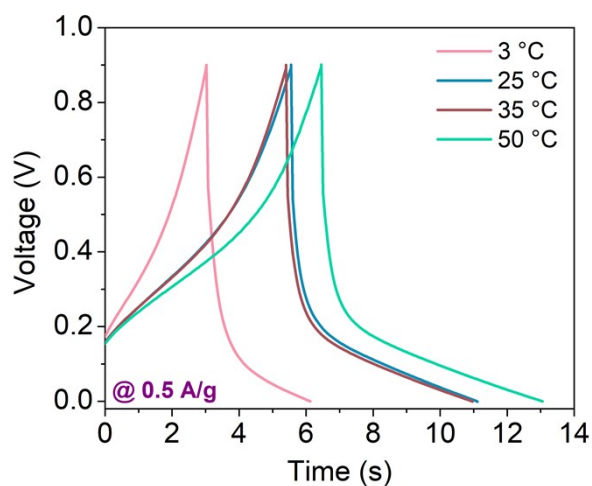


Figure S10. The GCD profile at 0.5 A/g current density of the flexible symmetric supercapacitor device, kept at different temperatures.

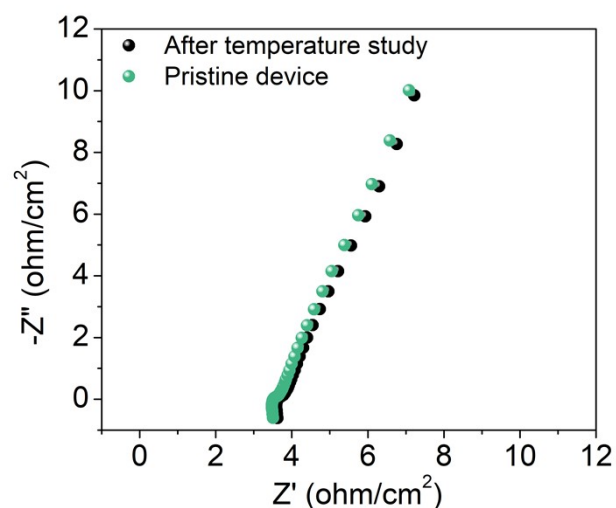


Figure S11. Nyquist plots of the pristine flexible supercapacitor device and the device after performing the measurements at various temperatures.

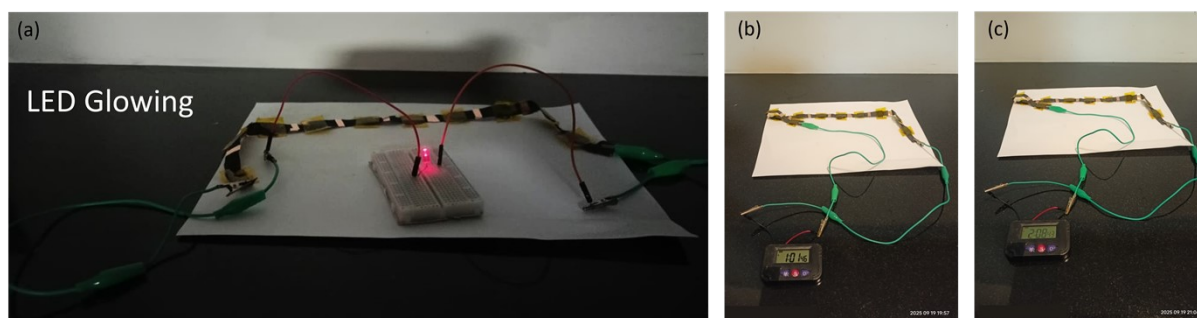


Figure S12. (a) LED glowing by connecting a series of flexible devices. A 1.2 V timer is running for almost 1 h, where (b) shows the start of the timer and (c) the LCD of it fades off.

Table S1. Comparison of the energy storage values with other literature.

Material	Electrode			Device			Reference
	Areal capacitance	Specific capacitance	Cyclic stability	Areal capacitance	Specific capacitance	Cyclic stability	
WO _{3-x} @TiO _{2-x} /P6 ICA	60.8 mF/cm ² at 5 mV/s	878.6 F/g at 0.1 mA/cm ²	3000	22 mF/cm ² at 0.3mA/cm ²	318 F/g at 0.3mA/cm ²	3000	1
WO _{3-x} /MoO _{3-x}	500 mF/cm ²	-	-	216 mF/cm ²	-	10,000 cycles	2
Sulfur-doped MoO _{3-x}	506 mF/cm ² at 10 mV/s	220 F/g at 10 mV/s	5000	-	-	-	3
TiO ₂ /MoO ₃	127.71 mF/cm ² at 0.6 mA/cm ²	3000	-	-	-	-	4
Mo _{0.11} W _{0.89} O _{3-x}	975 mF/cm ² at 5 mV/s	234 F/g at 5 A/g	1000	47 mF/cm ² at 5 mV/s	15.8 F/g at 0.1 A/g	10,000 cycles	This work

Reference

- 1 Q. Guo, Q. Li, L. Zheng, X. Xu and G. Nie, *ACS Appl Energy Mater*, 2022, **5**, 8443–8451.
- 2 X. Xiao, T. Ding, L. Yuan, Y. Shen, Q. Zhong, X. Zhang, Y. Cao, B. Hu, T. Zhai, L. Gong, J. Chen, Y. Tong, J. Zhou and Z. L. Wang, *Adv Energy Mater*, 2012, **2**, 1328–1332.
- 3 S. Liu, C. Xu, H. Yang, G. Qian, S. Hua, J. Liu, X. Zheng and X. Lu, *Small*, 2020, **16**, 1905778-1905785.
- 4 B. Zhang, S. Sun, N. Shi, X. Liao, G. Yin, Z. Huang, X. Chen and X. Pu, *J Alloys Compd*, 2020, **820**, 153066-153073.